

STYXL1 promotes malignant progression of hepatocellular carcinoma *via* downregulating CELF2 through the PI3K/Akt pathway

J.-Z. WU¹, N. JIANG¹, J.-M. LIN¹, X. LIU²

¹Department of Infectious Disease, Sichuan Academy of Medical Sciences and Sichuan Provincial People's Hospital, Chengdu, China

²Department of Pathology, Sichuan Academy of Medical Sciences and Sichuan Provincial People's Hospital, Chengdu, China

Abstract. – **OBJECTIVE:** This study was aimed to investigate the expression characteristics of STYXL1 in hepatocellular carcinoma (HCC), and to further analyze its regulatory role in promoting HCC development by targeting CELF2 to activate the phosphatidylinositol 3-kinase (PI3K)/protein kinase B (Akt) pathway.

PATIENTS AND METHODS: Expression levels of STYXL1 in 25 pairs of HCC tissue specimens and paracancerous normal ones collected from HCC patients were examined by quantitative Real Time-Polymerase Chain Reaction (qRT-PCR). Meanwhile, qRT-PCR was also performed to further verify the expression of STYXL1 in HCC cell lines. In addition, after STYXL1 knockdown model was constructed by lentivirus transfection in HCC cell lines Hep3B and Huh7, the Cell Counting Kit-8 (CCK-8), cell colony formation, 5-Ethynyl-2'-deoxyuridine (EdU), and flow cytometry assays were performed to analyze the influence of STYXL1 on HCC cell functions. Furthermore, an in-depth study of the relationship between STYXL1 and CELF2 was conducted to figure out the underlying mechanism.

RESULTS: The results of qRT-PCR revealed that the expression level of STYXL1 in HCC samples was remarkably higher than that in adjacent ones, and the difference was statistically significant. Compared with HCC patients with low expression of STYXL1, patients with high expression of STYXL1 had a higher overall survival rate. Similarly, the proliferation ability of HCC cells in sh-STYXL1 group remarkably decreased compared with controls, while the apoptosis ability was oppositely enhanced. In addition, Western Blotting results indicated that STYXL1 could elevate the expressions of PI3K/Akt pathway-related proteins. Meanwhile, a negative correlation between CELF2 and STYXL1 was identified in HCC tissues. Finally, the result of cell reverse experiments demonstrated that STYXL1 could affect the malignant progression of HCC *via* modulating CELF2 expression.

CONCLUSIONS: STYXL1 expression was remarkably upregulated in HCC tissues, as well as in cell lines. Its level was closely related to the poor prognosis of HCC patients. In addition, STYXL1 might be able to accelerate HCC proliferation rate and inhibit cell apoptosis *via* downregulating CELF2 through the PI3K/Akt pathway.

Key Words:

STYXL1, CELF2, Hepatocellular carcinoma (HCC), Proliferation.

Introduction

The incidence of hepatocellular carcinoma (HCC) has ranked fifth among common malignancies worldwide, and at least 1 million new cases have been diagnosed with each year^{1,2}. Due to the high infection rate of viral hepatitis B, the incidence of HCC in China is higher than the average in the world^{3,4}. According to the Global Cancer Report released by the World Health Organization, liver cancer accounts for 11.6% based on the incidence and composition of malignant tumors in China, ranking fourth. It accounts for 15.9% based on the mortality, ranking second^{4,5}. Since hepatic vascular metastasis can occur in the early phase of HCC, liver transplantation in the early stage of the tumor is an ideal treatment method⁶⁻⁸. Due to social factors and economic constraints, only a small number of patients in China can receive transplantation therapy. Therefore, surgical resection combined with chemotherapy has become the most important treatment^{8,9}. However, due to its low surgical resection rate, high recurrence rate, poor patient survival rate, and life quality, the overall treat-

ment effect is still unsatisfied^{10,11}. Therefore, it is of significance to uncover the pathogenesis of HCC, thus providing potential diagnostic markers and therapeutic intervention targets for HCC¹².

With the development of genetic testing technology, the large-scale genetic testing of clinical specimens, screening, and cloning of tumor-related genes have become possible^{13,14}. The human genome consists of approximately 3×10^9 base pairs, encoding approximately 30,000 genes. So far, 30 tumor-suppressor genes and more than 100 oncogenes have been identified¹⁵. Isolation and identification of tumor-associated genes, along with an analysis of the relationship between their abnormal expressions and tumor metastasis have become a hot topic in the research of tumor molecular biology¹⁶. However, unlike a few diseases with single-gene pathogenesis, more and more studies have shown that the occurrence, proliferation, and metastasis of HCC are associated with multiple oncogenes and tumor-suppressor genes that jointly regulate the occurrence and development of HCC^{17,18}. Through literature review, a potential role of STYXL1 in the development of tumor has been rarely reported^{19,20}. Therefore, in this study, we comprehensively analyzed the expression and biological roles of STYXL1 in HCC, and initially explored the molecular mechanism of its tumor regulation.

The phosphatidylinositol 3-kinase (PI3K) family is widely distributed in a variety of tissues and functions as Ser/Thr kinase and phosphatidylinositol kinase activity in different intracellular environments²¹. Protein kinase B (PKB), also known as AKT, constitutes the PI3K/Akt signaling pathway. It plays a pivotal role in inhibiting cell apoptosis, promoting cell proliferation and tumor formation in various tumors including HCC, and is involved in regulating tumor invasion and metastasis²¹. In recent years, CELF2, as a key protein in the PI3K/Akt pathway, has been studied in various tumors. This study investigated whether STYXL1 can promote the development of HCC by downregulating CELF2, and thus may provide experimental evidence for its clinical application.

Patients and Methods

Patients and HCC Samples

In this study, 25 pairs of HCC tissue specimens and their corresponding adjacent ones were surgically resected from HCC cases and stored

at -80°C . The collection of clinical specimens was approved by the Ethics Monitoring Committee. Patients and their families have been fully informed that their specimens would be used for scientific research. All participating patients signed informed consent.

Cell Lines and Reagents

Six human HCC cell lines (Bel-7402, HepG2, MHCC88H, SMMC-7221, Huh7, Hep3B) and one human normal liver cell line (LO2) were purchased from American Type Culture Collection (ATCC; Manassas, VA, USA). Dulbecco's Modified Eagle Medium (DMEM) medium and fetal bovine serum (FBS) were purchased from American Life Technologies (Gaithersburg, MD, USA). HCC cell lines were cultured with high-glucose DMEM containing 10% FBS, penicillin (100 U/mL) and streptomycin (100 $\mu\text{g}/\text{mL}$) at 37°C , in a 5% CO_2 incubator. The cells were passaged with 1% trypsin + EDTA for digestion when they reached the 80%-90% confluence.

Transfection

The negative control group (sh-NC) and the lentivirus containing the STYXL1 knockdown sequence (sh-STYXL1) were purchased from Shanghai GenePharma Company (Shanghai, China). The cells were plated in 6-well plates and grown to a cell density of 40%; then, transfection was performed according to the manufacturer's instructions. After 48 h, the cells were collected for quantitative Real Time-Polymerase Chain Reaction (qRT-PCR) analysis and cell function experiments.

Cell Counting Kit-8 (CCK-8) Assay

After 48 h of transfection, the cells were collected and plated into 96-well plates at 2000 cells per well. The cells were cultured for 24 h, 48 h, 72 h, and 96 h respectively, and then CCK-8 (Dojindo Laboratories, Kumamoto, Japan) reagent was added. After incubation for 2 hours, the optical density (OD) value of each well was measured in the microplate reader at 490 nm absorption wavelengths.

Colony Formation Assay

After 48 h of transfection, the cells were collected, and 200 cells were seeded in each well of a 6-well plate. The cells were cultured in complete medium for 2 weeks. The medium was changed once in the first week and then twice a week. After 2 weeks, visible colonies were fixed

in 2 mL of methanol for 20 minutes. After the methanol was aspirated, the cells were stained with 0.1% crystal violet staining solution for 20 minutes, washed 3 times with phosphate-buffered saline (PBS), photographed, and counted under a light-selective environment.

5-Ethynyl-2'-Deoxyuridine (EdU) Proliferation Assay

The EdU proliferation test (RiboBio, Nanjing, China) was performed according to the manufacturer's requirements. After transfection for 24 h, the cells were incubated with 50 μ M EdU for 2 h and stained with AdoLo and 4',6-diamidino-2-phenylindole (DAPI). The number of EdU-positive cells was detected by fluorescence microscopy. The EdU-positive ratio was calculated as the ratio of the number of EdU-positive cells to the total DAPI-labeled cells (blue cells).

Flow Cytometry Analysis of the Cell Apoptosis

The cells in the logarithmic growth phase were plated into 6-well plates. After 24 hours of drug treatment, the cells were collected, washed twice with PBS, and resuspended in the binding solution at room temperature for 15 min in the dark. Subsequently, the cells were incubated with 5 μ L of Annexin V-FITC (fluorescein isothiocyanate) and 5 μ L of Propidium Iodide (PI). The cell apoptosis rate was measured by flow cytometry (FACSCalibur; BD Biosciences, Detroit, MI, USA).

qRT-PCR

After the cells were accordingly treated, 1 mL of TRIzol (Invitrogen, Carlsbad, CA, USA) was used to lyse the cells, and the total RNA was extracted. The initially extracted RNA was treated with DNase I to remove genomic DNA and repurify the RNA. RNA reverse transcription was performed according to the Prime Script Reverse Transcription Kit (TaKaRa, Otsu, Shiga, Japan) instructions, followed by real time-PCR using the SYBR[®] Premix Ex Taq[™] kit (TaKaRa, Otsu, Shiga, Japan). PCR reaction was performed using the StepOne Plus Real-time PCR System (Applied Biosystems, Foster City, CA, USA). The following primers were used for qRT-PCR reaction: STYXL1: forward: 5'-CCG-CCATCATAGCCTACCT-3', reverse: 5'-CAATC-CCCGATTTGGACA-3'; CELF2: forward: 5'-CCCAGAATGCACTGCACAATA-3', reverse: 5'-GATCGGCATGAAACGCTTGAA-3';

glyceraldehyde 3-phosphate dehydrogenase (GAPDH): forward: 5'-GATTCACCCATGG-CAAATCC-3', reverse: 5'-TGGGATTTCCATT-GATGACAAG-3'. Three replicate wells were repeated for each sample, and the assay was repeated twice. The Bio-Rad PCR instrument was used to analyze and process the data with the software iQ5 2.0 (Bio-Rad, Hercules, CA, USA). GAPDH and U6 genes were used as internal references, and the gene expression was calculated by the 2^{- $\Delta\Delta$ Ct} method.

Western Blot

The transfected cells were lysed using cell lysis buffer, shaken on ice for 30 minutes, and centrifuged at 14,000 \times g for 15 minutes at 4°C. The total protein concentration was calculated by bicinchoninic acid (BCA) Protein Assay Kit (Pierce, Rockford, IL, USA). The extracted proteins were separated using a 10% sodium dodecyl sulphate-polyacrylamide gel electrophoresis (SDS-PAGE) and subsequently transferred to a polyvinylidene difluoride membrane (Millipore, Billerica, MA, USA). Western blot analysis was performed according to standard procedures. The primary antibodies against STYXL1, CELF2, PTEN, PI3K, AKT, and GAPDH, and the secondary antibodies were all purchased from Cell Signaling Technology (Danvers, MA, USA).

Statistically Analysis

Statistical analysis was performed using GraphPad Prism 5 V5.01 software (La Jolla, CA, USA). The differences between two groups were analyzed by using the Student's *t*-test. The comparison between multiple groups was done using One-way ANOVA test, followed by the post-hoc test (Least Significant Difference). Independent experiments were repeated at least three times for each experiment, and the data were expressed as average \pm standard deviation ($\bar{x} \pm s$). $p < 0.05$ was considered statistically significant (* $p < 0.05$, ** $p < 0.01$ and *** $p < 0.001$).

Results

STYXL1 Was Highly Expressed in HCC Tissues and Cell Lines

In order to determine the expression level of STYXL1 in HCC, a total of 25 pairs of tumor tissue samples and paracancerous ones of HCC patients were collected, and the expression difference of STYXL1 was detected by qRT-PCR.

The results showed that STYXL1 had a higher expression in HCC tissues than in paracancerous ones (Figure 1A), suggesting that STYXL1 may act as a cancer-promoting gene in HCC. In addition, the high expression of STYXL1 was found to be positively correlated with the pathological stage of HCC tissues (Figure 1B). Meanwhile, STYXL1 was found remarkably highly expressed in HCC cell lines compared to human normal liver cell line (LO2), and the difference was statistically significant (Figure 1C). According to the mRNA level of STYXL1, 25 pairs of tissue specimens were divided into high expression and low expression group, and the interplay between STYXL1 expression and the prognosis of HCC patients was analyzed. As shown in Figure 1D, high expression of STYXL1 was closely related to poor prognosis of HCC patients.

Knockdown of STYXL1 Inhibited Cell Proliferation, and Promoted Cell Apoptosis

To investigate the cellular functional changes of STYXL1 in HCC, the STYXL1 knock-

down lentiviral vector was constructed. After transfection of the STYXL1 knockdown vector in Hep3B and Huh7 cell lines, qRT-PCR was performed to verify the interference efficiency, and the difference was statistically significant (Figure 2A). Subsequently, CCK-8, colony formation, EdU, and flow cytometry assays were performed. The results indicated that the proliferation ability of HCC cells in the sh-STYXL1 group was significantly reduced compared with that in the sh-NC group (Figure 2B-2D). However, the cell apoptotic ability showed an opposite trend (Figure 2E).

Knockdown of STYXL1 Inactivated the PI3K/Akt Signaling Pathway

In order to investigate the correlation between STYXL1 and PI3K/Akt signaling pathway in HCC, Western blotting assay was performed. The result showed that the knockdown of STYXL1 could reduce the expression of the key factors including PTEN, PI3K, and AKT in the PI3K/Akt signaling pathway, and thus promoted the development of HCC (Figure 3).

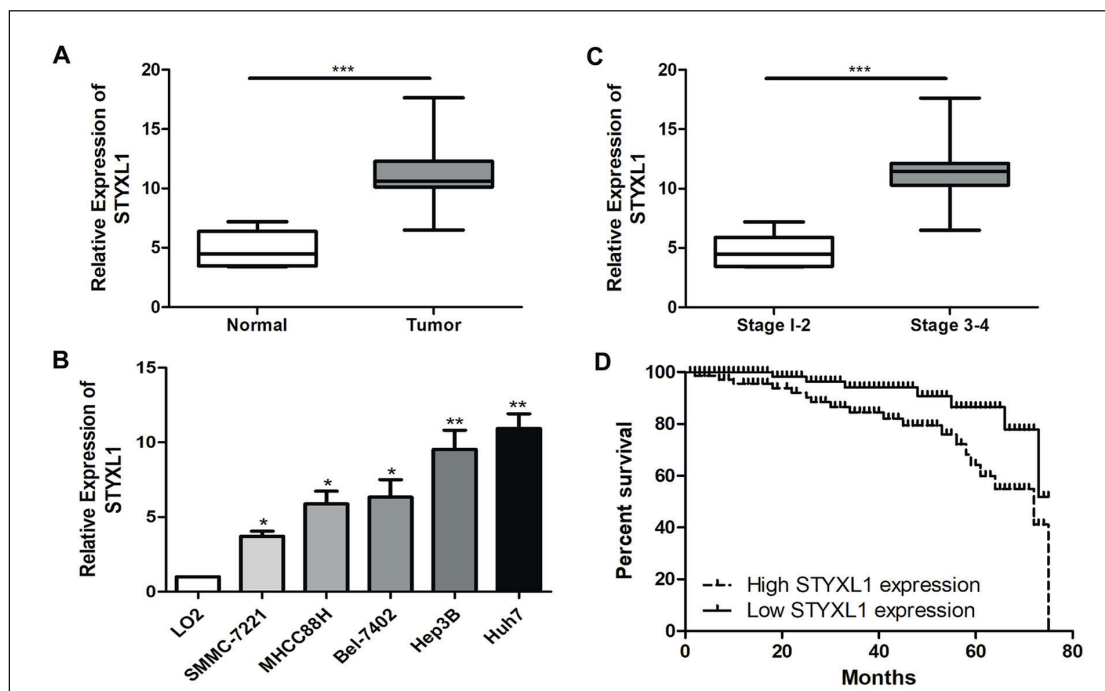


Figure 1. STYXL1 is highly expressed in hepatocellular carcinoma tissues and cell lines. **A**, qRT-PCR was used to detect the difference in expression of STYXL1 in hepatocellular carcinoma tumor tissues and adjacent tissues. **B**, qRT-PCR was used to detect the difference in the expression of STYXL1 in patients with different pathological stage hepatocellular carcinoma. **C**, qRT-PCR was used to detect the expression level of STYXL1 in hepatocellular carcinoma cell lines. **D**, Kaplan Meier survival curve of patients with hepatocellular carcinoma based on STYXL1 expression was shown; the prognosis of patients with high expression was significantly worse than that of low expression group. Data are mean ± SD, * $p < 0.05$, ** $p < 0.01$, *** $p < 0.001$.

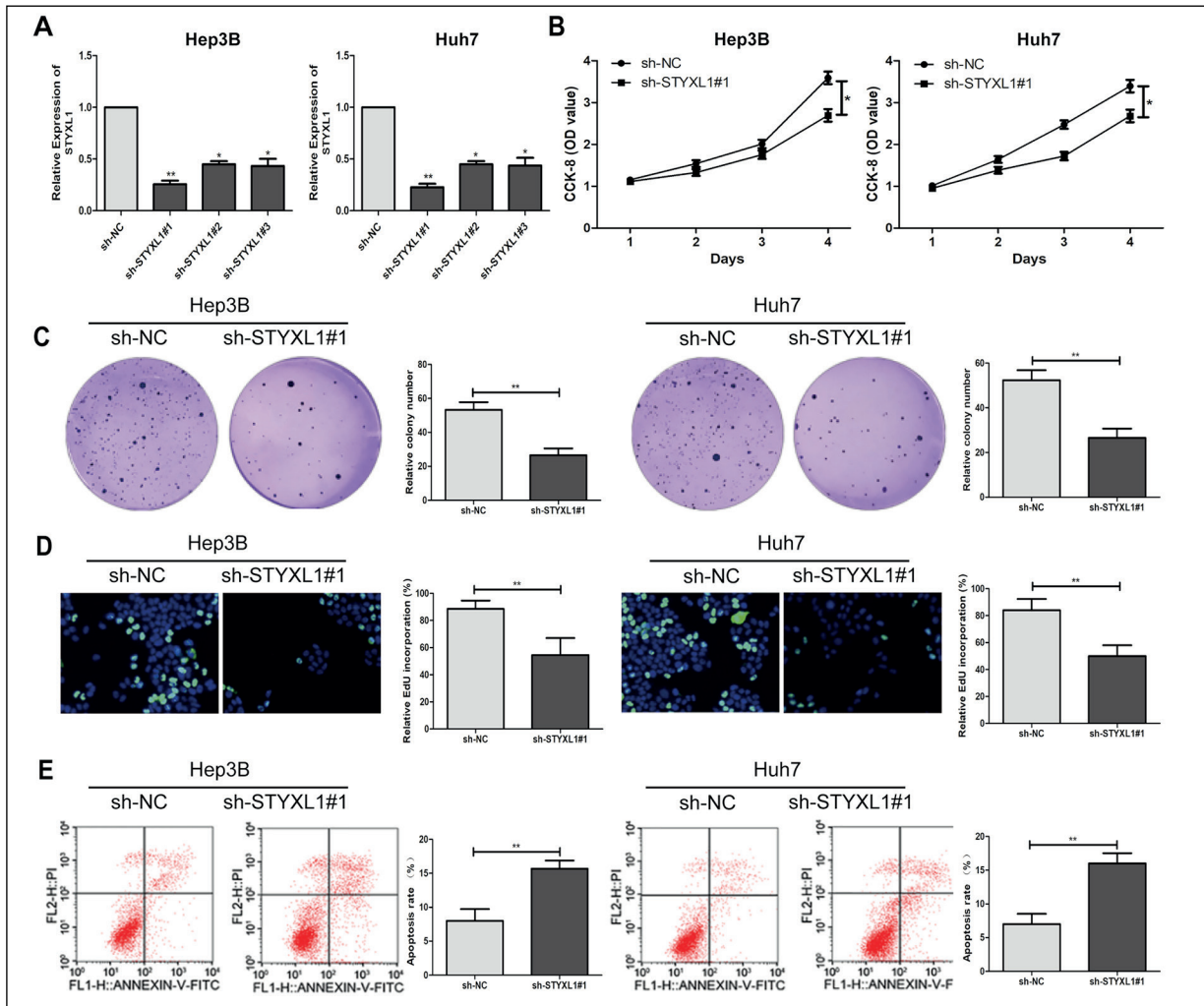


Figure 2. Silencing STYXL1 inhibits hepatocyte cancer cell proliferation and promotes apoptosis. **A**, qRT-PCR verified the interference efficiency of STYXL1 after transfection of STYXL1 knockdown vector in Hep3B and Huh7 cell lines. **B**, CCK-8 assay was performed to detect the effect of silencing STYXL1 on proliferation of hepatocellular carcinoma cells in Hep3B and Huh7 cell lines. **C**, Plate cloning experiment was performed to detect the effect of silencing STYXL1 on the number of hepatoma-positive proliferating cells in the Hep3B and Huh7 cell lines (magnification: 10 \times). **D**, The EdU assay was performed to detect the effect of silencing STYXL1 on proliferation of hepatocellular carcinoma cells in Hep3B and Huh7 cell lines (magnification: 40 \times). **E**, Flow cytometry assay was performed to detect the effect of silencing STYXL1 on apoptosis of hepatocellular carcinoma cells in Hep3B and Huh7 cell lines. Data are mean \pm SD, * p <0.05.

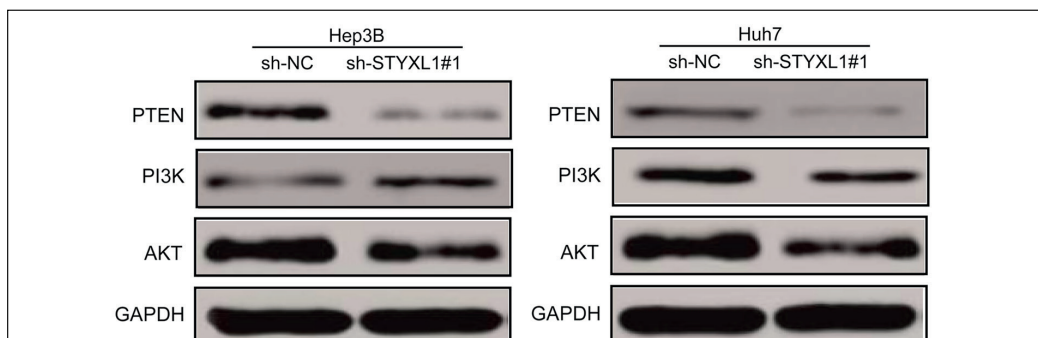


Figure 3. Silencing STYXL1 reduces the expression of PI3K/AKT signaling pathway-associated factors. Western Blotting assay was used to detect the expression of PTEN, PI3K, and AKT in PI3K/AKT signaling pathway in hepatocellular carcinoma cells after knockdown of STYXL1.

CELF2 Was Lowly Expressed in Hepatocellular Carcinoma Tissues and Cell Lines

After constructing the STYXL1 knockdown model in Hep3B and Huh7 cell lines, Western blotting was performed. The result revealed that compared with the control group, CELF2 expression was remarkably upregulated in the STYXL1 silencing group (Figure 4A), and STYXL1 expression was also elevated in the CELF2 silencing group (Figure 4B). In addition, the qRT-PCR result showed that the expression level of CELF2 in tumor tissues of HCC patients was significantly reduced compared with adjacent tissues, and the difference was statistically significant (Figure 4C). Next, it was found by qRT-PCR that CELF2 was conspicuously downregulated in HCC cell lines (Figure 4D). In addition, according to the mRNA expression of CELF2, 25 pairs of HCC tissue specimens and paracancerous ones were divided into high expression and low expression group. The relationship between CELF2 expression and prognosis of HCC patients was analyzed. As shown in Figure 4E, low expression of CELF2 was closely associated with poor prognosis of HCC patients. Additionally, the expressions of STYXL1 and CELF2 were detected by qRT-PCR, and the results showed that STYXL1 and CELF2 were negatively correlated in HCC tissues (Figure 4F).

CELF2 Modulated STYXL1 Expression in Hepatocellular Carcinoma Tissues and Cell Lines

To uncover the regulatory effect of STYXL1 on promoting the malignant progression of HCC, bioinformatics analysis was used to search for a potential relationship between STYXL1 and CELF2. After co-transfection of STYXL1 and CELF2 knockdown vectors in Hep3B and Huh7 cell lines, STYXL1 expression was detected by qRT-PCR (Figure 5A). Later, the results of CCK-8 and EdU experiments demonstrated that CELF2 could abolish the influence of STYXL1 on HCC proliferation ability (Figures 5B and 5C).

Discussion

Hepatocellular carcinoma (HCC) is commonly referred to as liver cancer. The mortality rate of HCC is the third-highest among all cancers in the world. The main cause of HCC-induced death

is the failure of early diagnosis and treatment, especially resistance to chemotherapy drugs and metastasis to other organs¹⁻⁶. Clinically, patients with the same diagnosis may have completely different processes and prognosis^{7,8}. Therefore, it is necessary to further study the mechanism of the occurrence and development of HCC, so as to achieve early detection, early diagnosis, and early treatment for affected patients⁹⁻¹².

The function of the PI3K/AKT signaling pathway in cells has been largely reported in literature^{21,22}. As the main energy metabolism regulation pathway in cells, it is not only closely related to the energy metabolism of cells, but also abnormally activated in various tumor cells. PI3K/AKT pathway is closely related to tumor cell proliferation, invasion and metastasis, chemical resistance, and radiation resistance. Drugs targeting this pathway have been well concerned in tumor treatment²². AKT, also known as protein kinase B (PKB), is a core protein of the PI3K/Akt signal transduction pathway. It was originally discovered as a proto-oncogene and has become a focus of attention because of its critical regulatory role in the metabolism, growth, proliferation, and protein synthesis of various cells^{23,24}. The activity of the PI3K/Akt signaling pathway is negatively regulated by the tumor-suppressor gene PTEN (a tumor suppressor lipophosphatase). As a PIP3-phosphatase, PTEN degrades PIP3 to PI-4,5-P2 by dephosphorylation, thereby blocking the efficient activation of Akt and its downstream effector molecules^{25,26}. PTEN plays a pivotal role in attenuating PIP3 signaling and upregulating PIP2 level, affecting multiple functional pathways of cells through methylation and ubiquitination²⁷. However, whether STYXL1 promotes the abnormal activation of the PI3K/AKT signaling pathway still remains elusive. In this study the result of the Western blotting showed that the knockdown of STYXL1 reduced the expressions of the key factors in the PI3K/AKT signaling pathway and inhibited the malignant progression of HCC.

Studies have shown that STYXL1 is highly expressed in gliomas¹⁹, and its high expression is associated with poor prognosis of patients. In addition, abnormally expressed STYXL1 is closely associated with poor prognosis in a variety of tumors^{19,20}. In the present study, the overexpression of STYXL1 was found to be able to promote the malignant progression of HCC. High level of STYXL1 predicted poor prognosis of HCC. In order to further study the molecular mechanism of

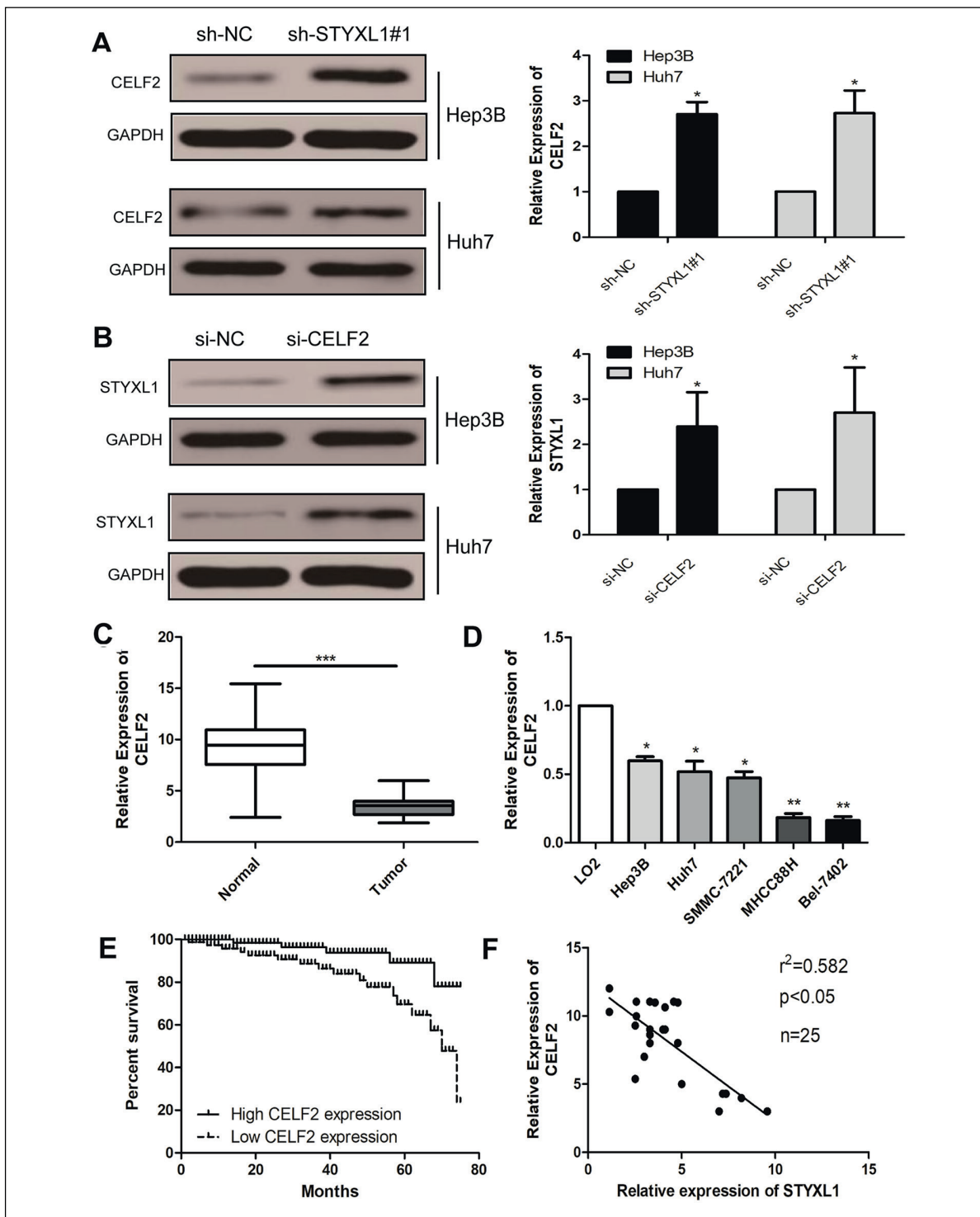


Figure 4. Interactions between STYXL1 and CELF2. **A**, Western blotting verified the expression level of CELF2 after transfection of STYXL1 knockdown vector in Hep3B and Huh7 cell lines. **B**, Western blotting verified the expression level of STYXL1 after transfection of CELF2 knockdown vector in Hep3B and Huh7 cell lines. **C**, qRT-PCR was used to detect the difference in the expression of CELF2 in tumor tissues and paracancerous tissues of patients with hepatocellular carcinoma. **D**, qRT-PCR was used to detect the expression level of CELF2 in hepatocellular carcinoma cell lines. **E**, Kaplan Meier survival curve of patients with hepatocellular carcinoma based on CELF2 expression was shown; the prognosis of patients with low expression was significantly worse than that of high expression group. **F**, There was a significant negative correlation between the expression levels of STYXL1 and CELF2 in hepatocellular carcinoma tissues. Data are mean \pm SD, * $p < 0.05$, ** $p < 0.01$, *** $p < 0.001$.

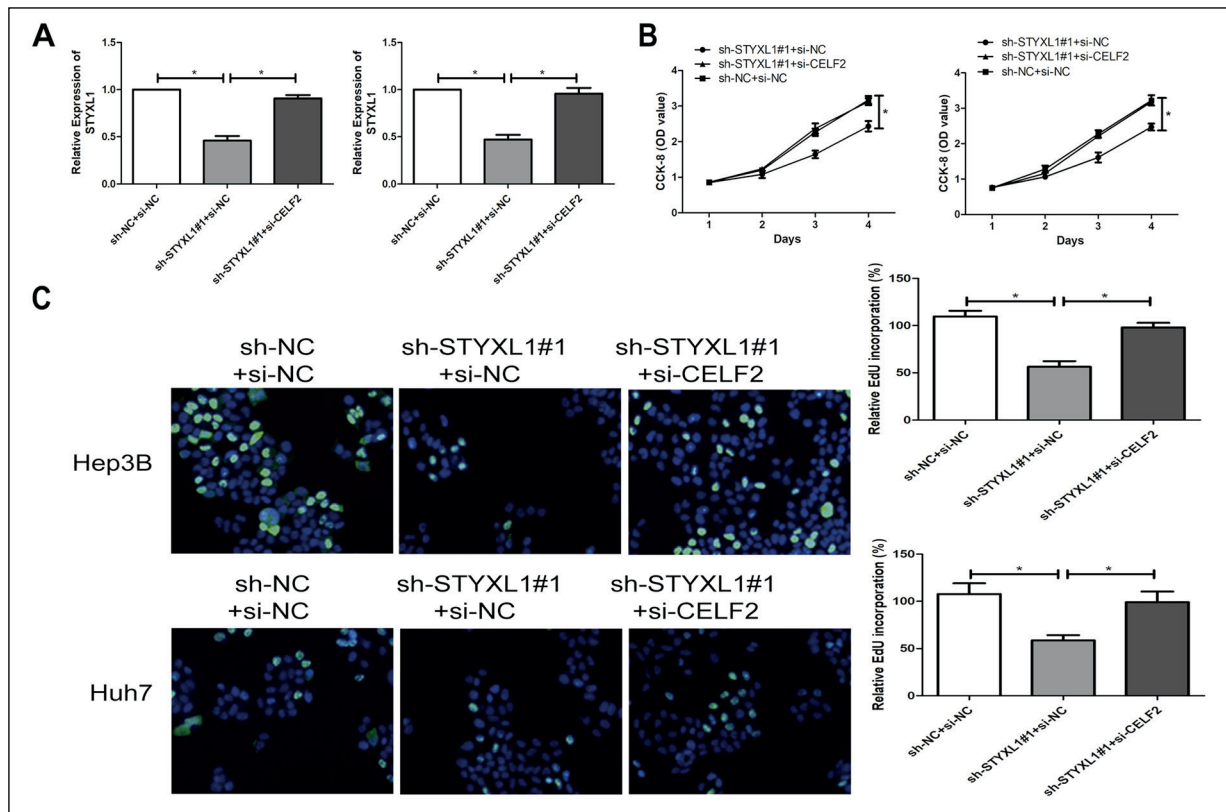


Figure 5. CELF2 regulates the expression of STYXL1 in hepatocellular carcinoma tissues and cell lines. **A**, The expression level of STYXL1 was detected after co-transfection of CELF2 and STYXL1 knockdown vectors in hepatocellular carcinoma cell lines by qRT-PCR. **B**, CCK-8 assay was used to detect the proliferation of hepatocyte cancer cells after co-transfection of CELF2 and STYXL1. **C**, The EDU assay was used to detect the effect of co-transfection of CELF2 and STYXL1 on the proliferation of hepatocellular carcinoma cells co-transfection (magnification: 40×). Data are mean ± SD, * $p < 0.05$.

STYXL1 in the development of HCC, the related cell *in vitro* experiments were performed. It was found that compared with the sh-NC group, the knockdown of STYXL1 in Hep3B and Huh7 cell lines inhibited the proliferation of HCC cells and promoted cell apoptosis.

Bioinformatics analysis predicted that CELF2 may interact with STYXL1. CELF2 was found to be lowly expressed in tumor tissues of HCC patients than in adjacent tissues, and CELF2 inhibited HCC cell proliferation. In addition, the expression levels of STYXL1 and CELF2 were negatively correlated in HCC cell lines. Based on the above findings, it was concluded that STYXL1 could act as a cancer-promoting gene, so as to promote HCC cell proliferation and inhibit cell apoptosis. In summary, STYXL1 might promote the proliferation of HCC and inhibit apoptosis by downregulating CELF2 through the PI3K/Akt pathway.

Conclusions

The expression of STYXL1 was found remarkably upregulated in HCC tissues and cell lines. STYXL1 was closely associated with the poor prognosis of HCC patients. In addition, STYXL1 might be able to promote HCC proliferation and inhibit apoptosis by downregulating CELF2 through the PI3K/Akt pathway.

Conflict of Interest

The Authors declare that they have no conflict of interests.

References

- 1) CLARK T, MAXIMIN S, MEIER J, POKHAREL S, BHARGAVA P. Hepatocellular carcinoma: review of epidemiology, screening, imaging diagnosis, response as-

- essment, and treatment. *Curr Probl Diagn Radiol* 2015; 44: 479-486.
- 2) MASSARWEH NN, EL-SERAG HB. Epidemiology of hepatocellular carcinoma and intrahepatic cholangiocarcinoma. *Cancer Control* 2017; 24: 1073274817729245.
 - 3) HUANG X, LI J, WANG F, HAO M. CT combined with tumor markers in the diagnosis and prognosis of hepatocellular carcinoma. *J BUON* 2018; 23: 985-991.
 - 4) MAK LY, CRUZ-RAMON V, CHINCHILLA-LOPEZ P, TORRES HA, LoCONTE NK, RICE JP, FOXHALL LE, STURGIS EM, MERRILL JK, BAILEY HH, MENDEZ-SANCHEZ N, YUEN MF, HWANG JP. Global epidemiology, prevention, and management of hepatocellular carcinoma. *Am Soc Clin Oncol Educ Book* 2018; 38: 262-279.
 - 5) BAECKER A, LIU X, LA VECCHIA C, ZHANG ZF. Worldwide incidence of hepatocellular carcinoma cases attributable to major risk factors. *Eur J Cancer Prev* 2018; 27: 205-212.
 - 6) GRANDHI MS, KIM AK, RONNEKLEIV-KELLY SM, KAMEL IR, GHASEBEH MA, PAWLIK TM. Hepatocellular carcinoma: from diagnosis to treatment. *Surg Oncol* 2016; 25: 74-85.
 - 7) BOYVAT F. Interventional radiologic treatment of hepatocellular carcinoma. *Exp Clin Transplant* 2017; 15: 25-30.
 - 8) EL-KHOUEIRY A. The promise of immunotherapy in the treatment of hepatocellular carcinoma. *Am Soc Clin Oncol Educ Book* 2017; 37: 311-317.
 - 9) ZHU ZX, HUANG JW, LIAO MH, ZENG Y. Treatment strategy for hepatocellular carcinoma in China: radiofrequency ablation versus liver resection. *Jpn J Clin Oncol* 2016; 46: 1075-1080.
 - 10) MORIS D, CHAKEDIS J, SUN SH, SPOLVERATO G, TSILIMIGRAS DI, NTANANIS-STATHOPOULOS I, SPARTALIS E, PAWLIK TM. Management, outcomes, and prognostic factors of ruptured hepatocellular carcinoma: A systematic review. *J Surg Oncol* 2018; 117: 341-353.
 - 11) KASSAHUN WT. Contemporary management of fibrolamellar hepatocellular carcinoma: diagnosis, treatment, outcome, prognostic factors, and recent developments. *World J Surg Oncol* 2016; 14: 151.
 - 12) EL JT, LAGANA SM, LEE H. Update on hepatocellular carcinoma: Pathologists' review. *World J Gastroenterol* 2019; 25: 1653-1665.
 - 13) PAHLE J, WALTHER W. Vectors and strategies for non-viral cancer gene therapy. *Expert Opin Biol Ther* 2016; 16: 443-461.
 - 14) HSIEHCHEN D, HSIEH A. Nearing saturation of cancer driver gene discovery. *J Hum Genet* 2018; 63: 941-943.
 - 15) OTOSHI T, NAGANO T, TACHIYARA M, NISHIMURA Y. Possible biomarkers for cancer immunotherapy. *Cancers (Basel)* 2019; 11: 935.
 - 16) MEREITER S, BALMANA M, CAMPOS D, GOMES J, REIS CA. Glycosylation in the era of cancer-targeted therapy: where are we heading? *Cancer Cell* 2019; 36: 6-16.
 - 17) AGARWAL R, NARAYAN J, BHATTACHARYYA A, SARASWAT M, TOMAR AK. Gene expression profiling, pathway analysis and subtype classification reveal molecular heterogeneity in hepatocellular carcinoma and suggest subtype specific therapeutic targets. *Cancer Genet* 2017; 216-217: 37-51.
 - 18) LIU KY, WANG LT, HSU SH, WANG SN. Homeobox genes and hepatocellular carcinoma. *Cancers (Basel)* 2019; 11. pii: E621.
 - 19) TOMAR VS, BARAL TK, NAGAVELU K, SOMASUNDARAM K. Serine/threonine/tyrosine-interacting-like protein 1 (STYXL1), a pseudo phosphatase, promotes oncogenesis in glioma. *Biochem Biophys Res Commun* 2019; 515: 241-247.
 - 20) FORTNER RT, DAMMS-MACHADO A, KAAKS R. Systematic review: tumor-associated antigen autoantibodies and ovarian cancer early detection. *Gynecol Oncol* 2017; 147: 465-480.
 - 21) CHEN Z, ZHOU ZY, HE CC, ZHANG JL, WANG J, XIAO ZY. Down-regulation of LncRNA NR027113 inhibits cell proliferation and metastasis via PTEN/PI3K/AKT signaling pathway in hepatocellular carcinoma. *Eur Rev Med Pharmacol Sci* 2018; 22: 7222-7232.
 - 22) CHEN Y, HUANG L, WANG S, LI JL, LI M, WU Y, LIU T. WFDC2 contributes to epithelial-mesenchymal transition (EMT) by activating AKT signaling pathway and regulating MMP-2 expression. *Cancer Manag Res* 2019; 11: 2415-2424.
 - 23) WU S, PENG L, SANG H, PING LQ, CHENG S. Anticancer effects of α -Bisabolol in human non-small cell lung carcinoma cells are mediated via apoptosis induction, cell cycle arrest, inhibition of cell migration and invasion and upregulation of P13K/AKT signalling pathway. *J BUON* 2018; 23: 1407-1412.
 - 24) XIN M, HE J, ZHANG Y, WU Y, YANG W, LIANG X, YIN X. Chinese herbal decoction of Wenshen Yangxue formula improved fertility and pregnancy rate in mice through PI3K/Akt signaling. *J Cell Biochem* 2019; 120: 3082-3090.
 - 25) DURMAZ I, GUVEN EB, ERSAHIN T, OZTURK M, CALIS I, CETIN-ATALAY R. Liver cancer cells are sensitive to Lanatoside C induced cell death independent of their PTEN status. *Phytomedicine* 2016; 23: 42-51.
 - 26) BITTINGER S, ALEXIADIS M, FULLER PJ. Expression status and mutational analysis of the PTEN and P13K subunit genes in ovarian granulosa cell tumors. *Int J Gynecol Cancer* 2009; 19: 339-342.
 - 27) LI L, ROSS AH. Why is PTEN an important tumor suppressor? *J Cell Biochem* 2007; 102: 1368-1374.